

substance: CrSb₂

property: physical properties

energy level scheme: Fig. 1.

energy gap

$E_{g,th}$	0.16 eV	from $\log \rho \propto E_g/2kT$, $T = 300...550$ K	56A, 57A
	(0.32 eV?)	from $\log \rho \propto E_g/2kT$, $T = 620...710$ K (the values given for σ at 669 and 710 K yield 0.45 eV. These large E_g figures may not be reliable since no kink is detectable on the thermopower curve, Fig. 3. Reproducibility of the measurements probably not checked on cooling)	56A, 57A
	0.14 eV	from $\log \rho \propto E_g/2kT$, $T = 200...260$ K	69A
	0.07 eV	from $\log \rho \propto E_g/2kT$, $T < 200$ K (see Fig. 2)	69A

resistivity: temperature dependence, Figs. 2, 3.

thermoelectric power: temperature dependence, Fig. 3.

Debye temperature

Θ_D	290 K	$T = 90$ K	maximum of Θ_D in the low-temperature region. from $C_p(T)$	78A
------------	-------	------------	--	-----

magnetic susceptibility

Curie-Weiss law, Fig. 4. $\chi(T)$ curves in [69A] falsified by oxidation of the samples [79K].

Néel temperature

T_N	273 K		from neutron-diffraction intensities	70H, 79K
	274 K		from heat capacity and magnetic susceptibility	78A, 79K

antiferromagnetic order

simple uniaxial type ($a_{\text{magn}} = a$, $b_{\text{magn}} = 2b$, $c_{\text{magn}} = 2c$), moments coupled ferromagnetically within (011) of the chemical cell, the moments in adjacent planes being antiparallel; moments perpendicular to b_{magn} [79K].

magnetic moments

p_A	1.94 μ_B	$T = 4$ K	from neutron diffraction (2 unpaired electrons/Cr, hence no Cr – Cr bonds)	70H, 79K
p_{eff}	3.1 μ_B	$T = 300...800$ K	from Curie-Weiss behavior with $\Theta_p = -500$ K	79K

peritectic temperature

T_{perit}	949 K			57A
	991.3 K		from heat capacity measurements	78A

heat capacity: temperature dependence: Figs. 5 and 6.

Comparative tables on structural data of transition metal dipnictides:

structure, chemical bond: see document ,

crystallographical data of compounds with octahedrally coordinated cations, see document ,

interatomic distances in marcasite- and loellingite-type compounds, see document .

References:

- 56A Abrikosov, N. Kh., Bankina, V. F.: Dokl. Akad. Nauk SSSR 108 (1956) 627.
- 57A Abrikosov, N. Kh.: Izv. Akad. Nauk SSSR, Ser. Fiz. 21 (1957) 141.
- 69A Adachi, K., Sato, K., Matsuura, M.: J. Phys. Soc. Japan 26 (1969) 906.
- 70H Holseth, H., Kjekshus, A., Andresen, A. F.: Acta Chem. Scand. 24 (1970) 3309.
- 72G Goodenough, J. B.: J. Solid State Chem. 5 (1972) 144.
- 78A Alles, A., Falk, B., Westrum, E. F., Gronvold, F.: J. Chem. Thermodyn. 10 (1978) 103.
- 79K Kjekshus, A., Peterzens, P. O., Rakke, T., Andresen, A. F.: Acta Chem. Scand. A33 (1979) 469.

Fig. 1.

CrSb_2 . Energy-level scheme for the loellingite-type antiferromagnet. The two non-bonding d electrons per Cr^{4+} ion occupy a localized ${}^3\text{A}(\text{b}^2)$ state [72G]. [n]: number of states per formula unit.

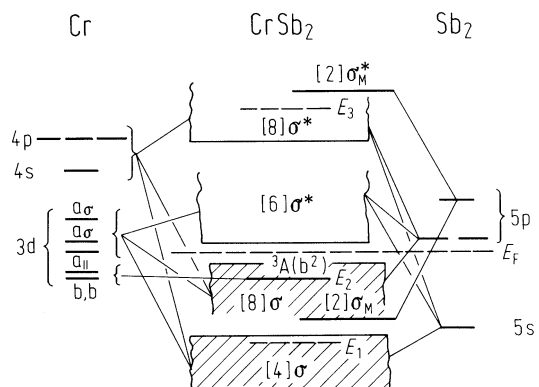


Fig. 2.

CrSb_2 . Electrical resistivity vs. reciprocal temperature for a sample quenched, crushed and annealed at 923 K [69A]. The broken curve represents the data of [57A].

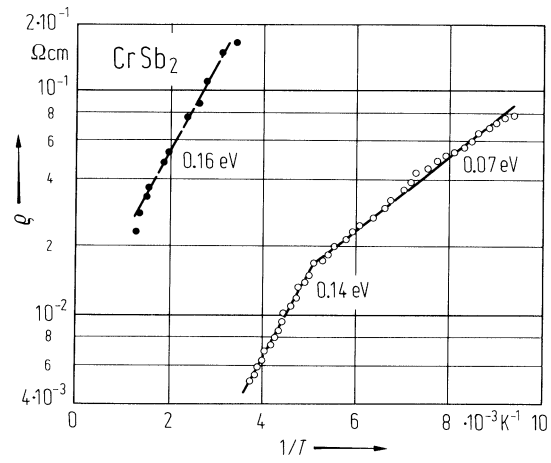


Fig. 3.

CrSb_2 . Thermoelectric power and resistivity vs. reciprocal temperature of polycrystalline samples [56A].

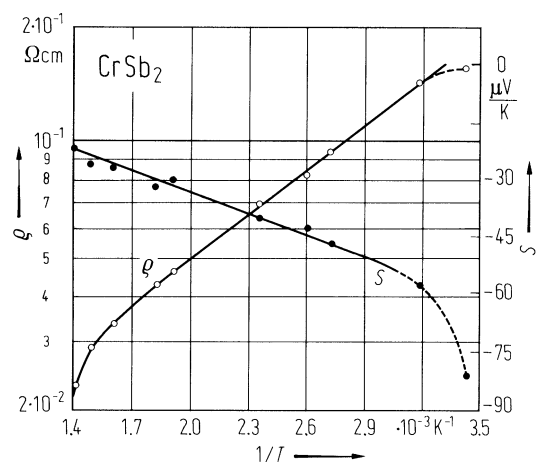


Fig. 4.

CrSb_2 . Reciprocal magnetic susceptibility vs. temperature [79K]. Measurements on powdered single crystals grown by a chlorine transport reaction. χ in CGS-emu.

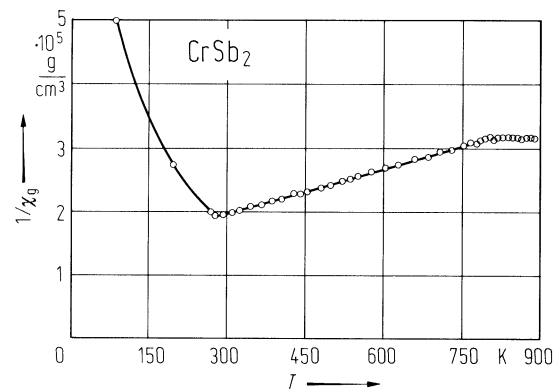


Fig. 5.

CrSb_2 . Heat capacity vs. temperature [78A]. For explanation of dashed line, see Fig. 6.

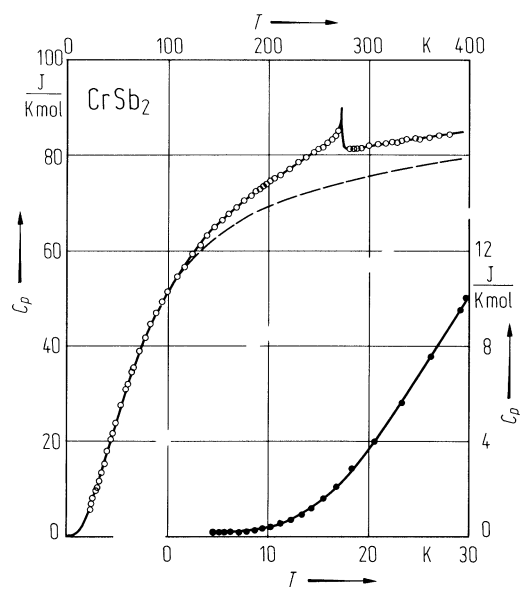


Fig. 6.

CrSb_2 . Heat capacity vs. temperature [78A]. Full curve: estimated vibrational contribution C_{vibr} . Broken curve: vibrational + dilatational (Nernst-Lindemann) contribution $C_{\text{vibr}} + C_{\text{dil}}$; $C_{\text{dil}} = AC_p^2 T_m/T$, with $A = 1.703 \cdot 10^{-3} \text{ K mol J}^{-1}$ and $T_m = 991.3 \text{ K}$, the peritectic temperature.

